

# High mass resolution ion microprobe analysis of rare earth elements in silicate glass, apatite and zircon: lack of matrix dependency

Yuji Sano<sup>a,b,\*</sup>, Kentaro Terada<sup>b</sup>, Takaaki Fukuoka<sup>c</sup>

<sup>a</sup>Center for Environmental Research, Ocean Research Institute, The University of Tokyo, Nakanoku, Tokyo 164-8639, Japan

<sup>b</sup>Department of Earth and Planetary Sciences, Faculty of Science, Hiroshima University, Kagami-yama 1-3, Higashi, Hiroshima 739-8526, Japan

<sup>c</sup>Department of Environmental Systems, Risho University, Kumagaya 360-0194, Japan

Received 22 December 2000; accepted 20 August 2001

## Abstract

The concentrations of all rare earth elements (REE: La, Ce, Pr, Nd, Sm, Eu, Gd, Tb, Dy, Ho, Er, Tm, Yb and Lu) in silicate glass, apatite and zircon were measured by an ion microprobe method with a high mass resolving power of 9300 at 1% peak height. Observed contents of REE in apatite extracted from a dacite agree well with those measured by the isotope dilution-thermal ionization mass spectrometry (ID-TIMS) method within 30% error at  $2\sigma$ . The contents of heavy REE in several zircons are consistent with those measured by ID-TIMS and instrumental neutron activation analysis (INAA), while the light REE abundances are significantly lower by ion microprobe than by the other methods. The discrepancy is partly due to the presence of 1–5- $\mu\text{m}$  inclusions of apatites within zircon crystals. Secondary ion yields of REE observed in a silicate glass show a very similar trend to those in apatite and zircon. Since the chemical composition of the silicate glass is appreciably different from the apatite and zircon, relative secondary ion yields of REE are probably independent from matrix effect, which is the most important finding of this work. Calculated partition coefficients of REE between melt and apatite agree well with reported values while the coefficients between melt and zircon are discrepant from those in literature. The REE coefficients in zircon increase with increase of the ionic radius logarithmically, suggesting power law dependence of the coefficients. © 2002 Elsevier Science B.V. All rights reserved.

**Keywords:** Ion microprobe; Rare earth element; Silicate glass; Apatite; Zircon

## 1. Introduction

There are several analytical methods capable of determining rare earth elements (REE) in rock and mineral samples with detection limits of ppm, including instrumental neutron activation analysis (INAA; Potts et al., 1973; Murali et al., 1983; Heaman et al.,

\* Corresponding author. Department of Earth and Planetary Sciences, Faculty of Science, Hiroshima University, Kagami-yama 1-3, Higashi, Hiroshima 739-8526, Japan. Tel.: +81-3-5351-6836; fax: +81-3-5351-6823.

E-mail address: ysano@ori.u-tokyo.ac.jp (Y. Sano).

1990), the isotope dilution method using a thermal ionization mass spectrometer after chemical dissolution and dissociation (ID-TIMS; Nagasawa, 1970; Kay and Gast, 1973; Fujimaki, 1986), inductively coupled plasma source-mass spectrometry using a laser-ablation sampling technique (LA-ICP-MS; Jackson et al., 1992; Perkins et al., 1993; Longerich et al., 1996) and secondary ion mass spectrometry (SIMS; Metson et al., 1984; MacRae and Metson, 1985; Zinner and Crozaz, 1986a,b; Fahey et al., 1987; Shimizu and Richardson, 1987). LA-ICP-MS and SIMS have the potential to detect sub-ppm level REE in situ and have a spatial resolution of less than 100  $\mu\text{m}$ . However, SIMS method is affected by the spectroscopic (isobaric) interference of light REE oxides onto the heavier REE and by matrix effects, while there is not a significant matrix problem in LA-ICP-MS method (Eggins et al., 1998). In SIMS studies using a CAMECA IMS 3f series instrument, the moderate energy filtering method is commonly used to overcome the interference problems (Zinner and Crozaz, 1986a,b; Grandjean and Albarede, 1989; Johnson et al., 1990; Hinton and Upton, 1991; Ireland and Wlotzka, 1992; references cited in Hoskin et al., 2000), but this causes a significant loss of secondary ion transmission, down to two orders of magnitude, which results in inadequate sensitivity. If both high mass resolution and high transmission are achieved at the same time using SIMS, the REE sensitivity would increase. The Sensitive High-Resolution Ion MicroProbe (SHRIMP) is capable of producing high transmission at high resolution and REE abundances have been measured using the high-resolution mode (Maas et al., 1992; Hoskin, 1998; Sano et al., 1999a; Sano and Terada, 2001). The primary purpose of this paper is to present a method for REE abundance measurement in a silicate glass and in the minerals apatite and zircon using SHRIMP. The relationship between REE secondary ion yields, ionization potential and the matrix effect will be discussed.

The partitioning of REE between two phases, mineral/melt has been intensively studied to understand their behavior and effects upon igneous processes since the 1970s (Nagasawa, 1970; Matsui et al., 1977). The partition coefficients of REE for apatite/melt were generally consistent with reported data while those for zircon/melt were sometime con-

troversial (Gromet and Silver, 1983; Fujimaki, 1986; Heaman et al., 1990). Hinton and Upton (1991) reported that the discrepancy in zircon partitioning was attributable to excess light REE in bulk analyses possibly affected by xenotime inclusions or areas of alteration within zircon. They further suggested that it is possible to estimate the REE concentrations in the melts by those in coexisting zircon even though the presence of other phases and effects on the partitioning due to physical changes such as temperature and pressure are ignored. Recently, Hoskin et al. (2000) argued that such back-calculation of REE composition of the original melt was successful in the case of apatite but not applicable for zircon. The second purpose of this paper is to give the partition coefficients of REE for apatite/melt and zircon/melt based on SHRIMP data and to verify the validity of back-calculation.

## 2. Experimental

Several small grains of apatite extracted from the Torihama dacite pyroclastic pumice collected from southern Kyushu, Japan (Ui, 1971), were mounted in an epoxy-resin disc together with a few grains of standard apatite "PRAP" and NIST SRM610 standard glass (approximately 500  $\mu\text{m} \times 1 \text{ mm}$ ). The PRAP was derived from an alkaline rock of the Prairie Lake circular complex in the Canadian Shield extensively used as a U/Pb and abundance calibration standard (Sano et al., 1999b). Several grains of the Torihama zircon were mounted in another epoxy disc together with a few grains of standard zircons SL13, QGNG and 91500, and the NIST 610 glass. SL13 is a Sri Lanka megacryst extensively used as a U/Pb and abundance calibration standard (Claoué-Long et al., 1995) and QGNG is a new multicrystal zircon standard from Quartz-Gabbro-Norite-Gneiss from Cape Donnington, South Australia. 91500 is a Canadian megacryst whose REE have been reported by other research groups (Wiedenbeck et al., 1995). Apatite and zircon grains were polished to provide a flat surface for sputtering of secondary ions until they were exposed through their midsections using 1  $\mu\text{m}$  diamond paste. They were checked by EPMA to locate inclusion-free homogeneous regions. Then their surface was finished by 0.25  $\mu\text{m}$

diamond paste and was coated by a thin gold coating to prevent charging of the sample surface by the primary beam.

The samples were set in the sample lock of SHRIMP II at the Department of Earth and Planetary Sciences, Hiroshima University and were evacuated overnight to reduce possible hydride interferences. Using Kohler illumination, a  $\sim 6$ -nA mass filtered  $O_2^-$  primary beam was used to sputter a 30- $\mu$ m diameter flat-bottomed crater and secondary positive ions were extracted by a 10-kV accelerating voltage for mass analysis. The ion source and collector slits were set to 60 and 50  $\mu$ m, respectively. A mass resolution of 9300 at 1% peak height was employed to separate heavy REE from oxide of light REE in the NIST 610 glass with adequate flat topped peaks (see Fig. 1. of Sano et al., 1999a). No apparent isobaric interferences were found in the mass range over  $^{139}\text{La}$  to  $^{175}\text{Lu}$  at a mass resolution of 9300. Approximate 30% transmission has been reported for high mass resolution condition (Sano et al., 1999a).

In the case of NIST 610 glass and zircon samples, the magnet was cyclically peak-stepped from mass 104 ( $^{104}\text{Si}_2\text{O}_3^+$ ) to mass 175 ( $^{175}\text{Lu}^+$ ), including the background and all significant REE isotopes ( $^{139}\text{La}^+$ ,  $^{140}\text{Ce}^+$ ,  $^{141}\text{Pr}^+$ ,  $^{143}\text{Nd}^+$ ,  $^{146}\text{Nd}^+$ ,  $^{147}\text{Sm}^+$ ,  $^{149}\text{Sm}^+$ ,  $^{151}\text{Eu}^+$ ,  $^{153}\text{Eu}^+$ ,  $^{155}\text{Gd}^+$ ,  $^{157}\text{Gd}^+$ ,  $^{159}\text{Tb}^+$ ,  $^{161}\text{Dy}^+$ ,  $^{163}\text{Dy}^+$ ,  $^{165}\text{Ho}^+$ ,  $^{166}\text{Er}^+$ ,  $^{167}\text{Er}^+$ ,  $^{169}\text{Tm}^+$ ,  $^{171}\text{Yb}^+$  and  $^{172}\text{Yb}^+$ ). In the case of apatite samples, mass 159 for  $\text{Ca}_2\text{PO}_3^+$  was measured instead of  $^{104}\text{Si}_2\text{O}_3^+$ . Note that  $\text{Ca}_2\text{PO}_3^+$  was well resolved from  $^{159}\text{Tb}^+$ . Secondary ions were detected by means of an electron multiplier operating in the ion-counting mode. Peaks were counted for 40 s, resulting in single scans through the spectrum taking  $\sim 20$  min. A complete run comprising seven scans takes 2 h.

The PRAP apatite was crushed and then dissolved by  $\text{HNO}_3$  and HF. After adding indium as an internal standard, all REE contents in the solution were measured by ICP-MS. The precision of the REE measurements was estimated by repeated analyses of standard solution, and was found to be about  $\pm 5\%$  at

Table 1

Concentration, isotope abundance and isotope concentration of REEs in the NIST 610 standard glass, observed  $A^+/\text{Si}_2\text{O}_3^+$  ratios and secondary ion yield

Element	Mass	Concentration (ppm)	Isotope abundance	Isotope concentration (ppm)	$A^+/\text{Si}_2\text{O}_3^+$	Secondary ion yield
La	139	400	0.99911	400	27.2	0.0681
Ce	140	422	0.8848	373	21.9	0.0586
Pr	141	423	1	423	28.8	0.0680
Nd	143	397	0.1214	48.2	3.74	0.0775
Nd	146	397	0.1726	68.5	5.51	0.0804
Sm	147	412	0.1507	62.1	5.64	0.0908
Sm	149	412	0.1384	57.0	5.23	0.0917
Eu	151	415	0.4777	198	20.8	0.1048
Eu	153	415	0.5223	217	22.3	0.1027
Gd	155	421	0.1473	62.0	3.53	0.0569
Gd	157	421	0.1568	66.0	3.64	0.0551
Tb	159	413	1	413	22.5	0.0545
Dy	161	406	0.1888	76.7	4.56	0.0594
Dy	163	406	0.2497	101	5.95	0.0587
Ho	165	419	1	419	23.0	0.0548
Er	166	417	0.3341	139	6.73	0.0483
Er	167	417	0.2294	95.7	4.71	0.0492
Tm	169	415	1	415	21.0	0.0506
Yb	171	421	0.1431	60.2	3.15	0.0523
Yb	172	421	0.2182	91.9	5.17	0.0562
Lu	175	407	0.974	396	11.3	0.0285

Reproducibility of  $A^+/\text{Si}_2\text{O}_3^+$  ratios is less than 20% at  $2\sigma$ .

1 $\sigma$ . The accuracy of the measurements was verified by EPMA using La, Ce and Nd concentrations since they are abundant enough to analyze precisely. The concentrations of 10 REE (Ce, Nd, Sm, Eu, Tb, Dy, Ho, Tm, Yb and Lu) of a single grain of QGNG and Torihama zircon were measured by instrumental neutron activation analysis. Calibration was made against NIST 610 glass. Experimental details were given elsewhere (Fukuoka et al., 1987).

### 3. Results

Quantitative REE analysis requires either good calibration standards, which are not easily available, or knowledge about relevant secondary ion yields, in order to convert the observed peak intensities into concentrations. Seven spot measurements of NIST 610 glass were carried out to check the secondary

ion yields of all REE in silicate glass matrix. The  $^{104}\text{Si}_2\text{O}_3^+$  beam was used as an internal standard. Table 1 lists the observed ratio of ( $\text{A}^+ / ^{104}\text{Si}_2\text{O}_3^+$ ), the REE isotope concentrations calculated from the REE concentrations in literature (Reed, 1992) and stable isotopic composition when there are more than two isotopes. The secondary ion yields were obtained by dividing  $\text{A}^+ / ^{104}\text{Si}_2\text{O}_3^+$  by the concentration of A in the target. The precision of the yields is less than 20% at 2 $\sigma$ , estimated by the reproducibility of  $\text{A}^+ / ^{104}\text{Si}_2\text{O}_3^+$  ratios, which is consistent with the error calculated by ion counting statistics. Those of relative abundances of REE such as  $\text{La}^+ / \text{Sm}^+$  ratio are about 10% at 2 $\sigma$ . The secondary ion yields vary significantly from 0.0285 for Lu to 0.1027 and 0.1048 for Eu, even though the chemical properties of the REE are generally similar when compared with other elements. Note that isotopes of the same element such as Nd, Sm, and Eu show identical secondary ion

Table 2  
Concentration, isotope abundance and isotope concentration of REEs in PRAP standard apatite, observed  $\text{A}^+ / \text{Ca}_2\text{PO}_3^+$  ratios and secondary ion yield

Element	Mass	Concentration <sup>a</sup> (ppm)	Isotope abundance	Isotope concentration (ppm)	$\text{A}^+ / \text{Ca}_2\text{PO}_3^+$	Secondary ion yield
La	139	4870	0.99911	4866	2.33	0.000479
Ce	140	11,300	0.8848	9998	2.90	0.000290
Pr	141	1414	1	1414	0.597	0.000422
Nd	143	5450	0.1214	662	0.357	0.000540
Nd	146	5450	0.1726	941	0.504	0.000536
Sm	147	999	0.1507	151	0.0876	0.000582
Sm	149	999	0.1384	138	0.0801	0.000579
Eu	151	258	0.4777	123	0.0884	0.000716
Eu	153	258	0.5223	135	0.0972	0.000720
Gd	155	706	0.1473	104	0.0313	0.000301
Gd	157	706	0.1568	111	0.0322	0.000291
Tb	159	90.7	1	90.7	0.0174	0.000192
Dy	161	371	0.1888	70.0	0.0188	0.000269
Dy	163	371	0.2497	92.6	0.0241	0.000260
Ho	165	54.2	1	54.2	0.0128	0.000236
Er	166	115	0.3341	38.4	0.00726	0.000189
Er	167	115	0.2294	26.4	0.00506	0.000192
Tm	169	13.9	1	13.9	0.00227	0.000164
Yb	171	67.1	0.1431	9.60	0.00178	0.000186
Yb	172	67.1	0.2182	14.6	0.00268	0.000183
Lu	175	8.08	0.974	7.87	0.000319	0.0000405

Reproducibility of  $\text{A}^+ / \text{Ca}_2\text{PO}_3^+$  ratios is less than 20% at 2 $\sigma$ .

<sup>a</sup> REE concentrations obtained by solution ICP-MS on a separate aliquot. Precision is 5% (1 $\sigma$ ).

yields within the reproducibility of <20%. The trend of the yield variation, high in middle REE and very low in Lu, agrees well with that obtained for NIST 612 glass using SHRIMP (Sano et al., 1999a).

Six spot measurements of PRAP standard apatite were carried out to obtain the secondary ion yields of REE in apatite matrix. The  $^{159}\text{Ca}_2\text{PO}_3^+$  beam was used as an internal standard. Table 2 lists the observed ratio of ( $\text{A}^+ / ^{159}\text{Ca}_2\text{PO}_3^+$ ), the REE isotope concentrations calculated from the REE contents measured by ICP-MS and stable isotopic composition when there are more than two isotopes. The secondary ion yields were obtained using the ratio of  $\text{A}^+ / ^{159}\text{Ca}_2\text{PO}_3^+$  to the REE isotope concentration. The precision of the yields is less than 20% at  $2\sigma$ , estimated using the reproducibility of  $\text{A}^+ / ^{159}\text{Ca}_2\text{PO}_3^+$  ratios. Again relative REE abundances are about 10% at  $2\sigma$ . The REE secondary ion yields vary significantly from

0.0000405 for Lu to 0.000716 and 0.000720 for Eu. These values are consistent with the yields found in a preliminary study (Sano and Terada, 2001).

Six spot measurements of SL13 standard zircon were carried out to check the secondary ion yields of REE in a zircon matrix. As in the analysis of the glass,  $^{104}\text{Si}_2\text{O}_3^+$  was used as an internal standard. Table 3 lists the observed ratio ( $\text{A}^+ / ^{104}\text{Si}_2\text{O}_3^+$ ), the REE isotope concentrations calculated from literature data (Ireland and Wlotzka, 1992) and stable isotopic composition when there are more than two isotopes. The secondary ion yields were obtained using the ratio of  $\text{A}^+ / ^{104}\text{Si}_2\text{O}_3^+$  to the REE isotope concentration. Precisions of the La, Pr, Nd and Sm yields are 30–40% at  $2\sigma$  estimated using the reproducibility of  $\text{A}^+ / ^{104}\text{Si}_2\text{O}_3^+$  ratios. Precision of other REE are less than 20% at  $2\sigma$  and relative abundance ratios are about 10% at  $2\sigma$ . Poor reproducibility of the light

Table 3

Concentration, isotope abundance and isotope concentration of REEs in SL13 standard zircon, observed  $\text{A}^+ / \text{Si}_2\text{O}_3^+$  ratios and secondary ion yield

Element	Mass	Concentration <sup>a</sup> (ppm)	Isotope abundance	Isotope concentration (ppm)	$\text{A}^+ / \text{Si}_2\text{O}_3^+$	Secondary ion yield
La	139	0.012	0.99911	0.0120	0.00247	0.2061
Ce	140	0.43	0.8848	0.380	0.0356	0.0935
Pr	141	0.014	1	0.0140	0.00224	0.1601
Nd	143	0.11 <sup>b</sup>	0.1214	0.0132	0.00188	0.1430
Nd	146	0.11 <sup>b</sup>	0.1726	0.0187	0.00257	0.1370
Sm	147	0.087	0.1507	0.0131	0.00354	0.2699
Sm	149	0.087	0.1384	0.0120	0.00335	0.2784
Eu	151	0.064	0.4777	0.0306	0.00630	0.2062
Eu	153	0.064	0.5223	0.0334	0.00696	0.2082
Gd	155	0.63	0.1473	0.0928	0.0127	0.1370
Gd	157	0.63	0.1568	0.0988	0.0138	0.1393
Tb	159	0.32	1	0.320	0.0329	0.1030
Dy	161	4.9	0.1888	0.925	0.104	0.1120
Dy	163	4.9	0.2497	1.22	0.135	0.1106
Ho	165	1.7	1	1.70	0.192	0.1129
Er	166	9.6	0.3341	3.21	0.311	0.0971
Er	167	9.6	0.2294	2.20	0.203	0.0923
Tm	169	2	1	2.00	0.244	0.1222
Yb	171	19	0.1431	2.72	0.452	0.1664
Yb	172	19	0.2182	4.15	0.692	0.1669
Lu	175	5	0.974	4.87	0.219	0.0449

Reproducibility of  $\text{La}^+ / \text{Si}_2\text{O}_3^+$ ,  $\text{Pr}^+ / \text{Si}_2\text{O}_3^+$ ,  $\text{Nd}^+ / \text{Si}_2\text{O}_3^+$  and  $\text{Sm}^+ / \text{Si}_2\text{O}_3^+$  ratios is 30–40% at  $2\sigma$ . Those of the other elements are less than 20%.

<sup>a</sup> Concentrations in the SL13 zircon from Ireland and Wlotzka (1992).

<sup>b</sup> Estimated by  $\text{Pr}^{2/3} \times \text{Sm}^{1/3}$  in chondrite normalized pattern.

Table 4  
Observed REEs concentrations in apatite and zircon grains measured by SHRIMP

Element	Torihama apatite (ppm)	Torihama zircon (ppm)	QGNG zircon (ppm)	91500 zircon (ppm)
La	778	0.011 ± 0.008	0.088 ± 0.043	0.014 ± 0.011
Ce	2040	15.3 ± 3.8	39.2 ± 5.9	2.59 ± 0.43
Pr	266	0.072 ± 0.037	0.37 ± 0.19	0.035 ± 0.015
Nd	1160	1.15 ± 0.20	5.0 ± 1.2	0.295 ± 0.064
Sm	242	2.10 ± 0.52	8.2 ± 1.4	0.278 ± 0.084
Eu	22.6	0.50 ± 0.12	0.74 ± 0.23	0.191 ± 0.065
Gd	221	13.86 ± 3.00	39.4 ± 8.2	1.60 ± 0.39
Tb	34.2	7.0 ± 1.6	17.2 ± 3.7	0.75 ± 0.20
Dy	184	111 ± 23	230 ± 43	12.3 ± 2.5
Ho	35.5	46 ± 11	75 ± 17	5.1 ± 1.4
Er	101	241 ± 48	340 ± 75	28.6 ± 6.2
Tm	15.3	57 ± 12	75 ± 14	7.5 ± 1.8
Yb	95.3	560 ± 110	620 ± 140	77 ± 18
Lu	12.9	127 ± 24	109 ± 21	17.1 ± 3.8
Sum REEs	5200	1180	1550	154
Ce/Ce*	1.08	132	53	33
Eu/Eu*	0.297	0.284	0.125	0.873
Lu/La	0.017	11600	1230	1260

Error in the concentration is  $2\sigma$  calculated from 5–6 successive measurements of different spots. Errors of Torihama apatite REEs are less than 30% at  $2\sigma$ .

REE is probably attributable to the low abundances of these elements,  $\sim 10$  ppb in SL13 zircon. The secondary ion yields vary significantly from 0.0449 for Lu to 0.2699 and 0.2784 for Sm.

Based on the secondary ion yields of REE in apatite and zircon matrix, we have measured all REE in Torihama apatite and a few zircons, Torihama, QGNG and 91500. Table 4 lists the abundance of REE in these samples together with total REE contents, Ce/Ce\* and Eu/Eu\* ratios, where Ce\* and Eu\* are estimated by  $\text{La}^{1/2} \times \text{Pr}^{1/2}$  and  $\text{Sm}^{1/2} \times \text{Gd}^{1/2}$  in chondrite normalized pattern, respectively, and Lu/La ratios. Precision of REE abundances in Torihama apatite are less than 30% at  $2\sigma$ , which were calculated by the combination of the error of secondary ion yields in Table 2 and reproducibility of  $\text{A}^{+}/^{159}\text{Ca}_2\text{PO}_3^{+}$  ratios in the sample. Errors assigned to the REE contents in zircon samples are estimated by the same procedure. Again poor precisions of La and Pr abundances in zircon may be due to their low concentrations.

Enrichment of heavy REE with increasing mass number, positive Ce anomaly and negative Eu anomaly in chondrite normalized patterns, are common features of terrestrial zircon samples (Hinton and Upton, 1991; Kinny et al., 1991; Ireland and

Wlotzka, 1992). This is the case for present samples, but total abundance of REE and La/Lu ratios vary significantly.

## 4. Discussion

### 4.1. Comparison of REE measurements

Nagasawa (1970) reported concentrations of nine REE (Ce, Nd, Sm, Eu, Gd, Dy, Er, Yb and Lu) in Torihama apatite, measured by ID-TIMS. Fig. 1 shows the comparison of the REE abundances measured by SHRIMP and ID-TIMS. In the wide dynamic range of 10–2000 ppm, SHRIMP data agree well with those by ID-TIMS within experimental errors. A correlation coefficient of 0.9998 suggests both data sets are identical. Therefore, the accuracy and precision of SHRIMP high-resolution REE measurements of apatite, within  $\pm 30\%$  at  $2\sigma$  is verified.

Fig. 2a, b and c indicates REE abundance patterns of measured zircon normalized to C1 chondrite (Anders and Grevesse, 1989) together with those in literature. Observed abundances of heavy REE from Dy to Lu in Torihama (Fig. 2a) and QGNG (Fig. 2b)

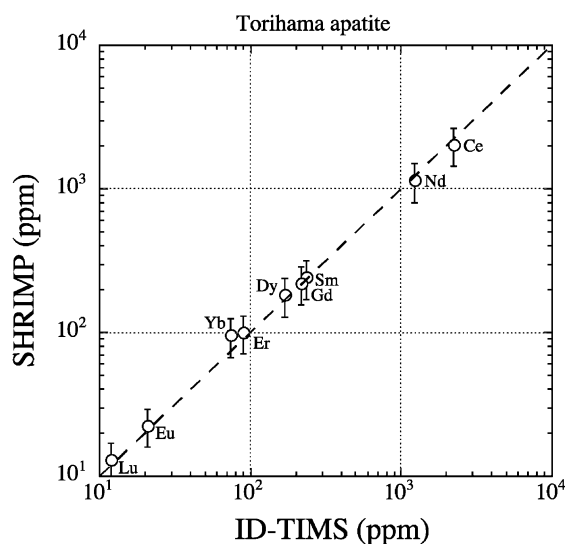


Fig. 1. Comparison of REE abundances in the Toriyama apatite measured by ID-TIMS (Nagasawa, 1970) and SHRIMP (this work). Data agree well with each other within experimental error of  $\pm 30\%$  at  $2\sigma$ .

zircons are consistent with those measured by bulk analytical methods, ID-TIMS (Nagasawa, 1970) and INAA. On the other hand, light REE such as Ce, Nd and Sm are higher in the bulk methods than by SHRIMP. SIMS data of 91500 zircon (Wiedenbeck et al., 1995) are generally consistent with SHRIMP data (Fig. 2c). A discrepancy for light REE between bulk measurements and SIMS analysis of zircon was reported by Kinny et al. (1991) and Hinton and Upton (1991). They suggested that this was due to the presence of inclusions with some light REE contents, such as apatite and xenotime or alteration resulting from damaged by radioactive decay of U and Th within the zircon. Fig. 3 shows electron backscatter images of Toriyama zircon grains. We found several tiny (1–5  $\mu\text{m}$ ) inclusions of apatite and glass, but no xenotime. Since the REE pattern of Toriyama apatite is much flatter than that of zircon, and abundances of light REE in the apatite are 3–4 orders of magnitude larger than those in the zircon, incorporation of tiny apatites could produce the observed differences between bulk and spot analyses (Fig. 2a). We have measured chemical compositions of glass inclusions by EPMA and they are very similar to those of groundmass (Nagasawa, 1970), suggesting that the

REE abundance of the glass is similar to those of groundmass and is 1–2 orders of magnitude smaller than that of apatite. Glass would, therefore, not contribute significantly to the pattern of bulk zircon. Note that even though QGNG zircon is used as a working standard for U/Pb calibration, the REE variations obtained by different analytical methods (Fig. 2b) suggests the presence of mineral inclusions in this zircon also. Therefore, it is essential to locate inclusion-free homogeneous regions in all zircon grains by EPMA before SHRIMP analysis.

#### 4.2. Secondary ion yields of REE in glass, apatite and zircon

Secondary ion yields are necessary to convert the observed peak intensities into concentrations. If matrix effects are significant, a good matrix-matched calibration standard is required. Reed (1983) reported secondary ion yields of REE relative to  $\text{Ca}^+$  in silicate glasses, showing significant variation by factors of 6–7, from 0.12 for Lu to 0.81 for Eu. A similar trend was reported by Zinner and Crozaz (1986a,b). The REE secondary ion yields of NIST 610 glass obtained here are consistent with those of Reed (1983) and Zinner and Crozaz (1986a,b), even though absolute yields are different because we used  $^{104}\text{Si}_2\text{O}_3^+$  as the internal standard. No systematic relation appears to exist between the secondary ion yields and physical characteristics of REE such as ionic radius and electronegativity. Based on the local thermal equilibrium (LTE) model (Andersen and Hinthorne, 1973) as applied to secondary ion production, Reed (1983) derived the following equation.

$$\frac{n_{M^+}}{n_M} = \text{const} \times \frac{T^{3/2}}{n_{e^-}} \frac{B_{M^+}}{B_M} e^{-I_M/kT} \quad (1)$$

where  $T$  is the plasma temperature in K,  $n$  is the number of atoms, ions and electrons,  $B$  the partition function of the atoms or ions and  $I_M$  is the ionisation potential. Then relative secondary ion yields of REE are probably a function of the ionisation potential as follows.

$$\frac{S_A}{S_B} = \text{const} \times e^{(I_B - I_A)/kT} \quad (2)$$

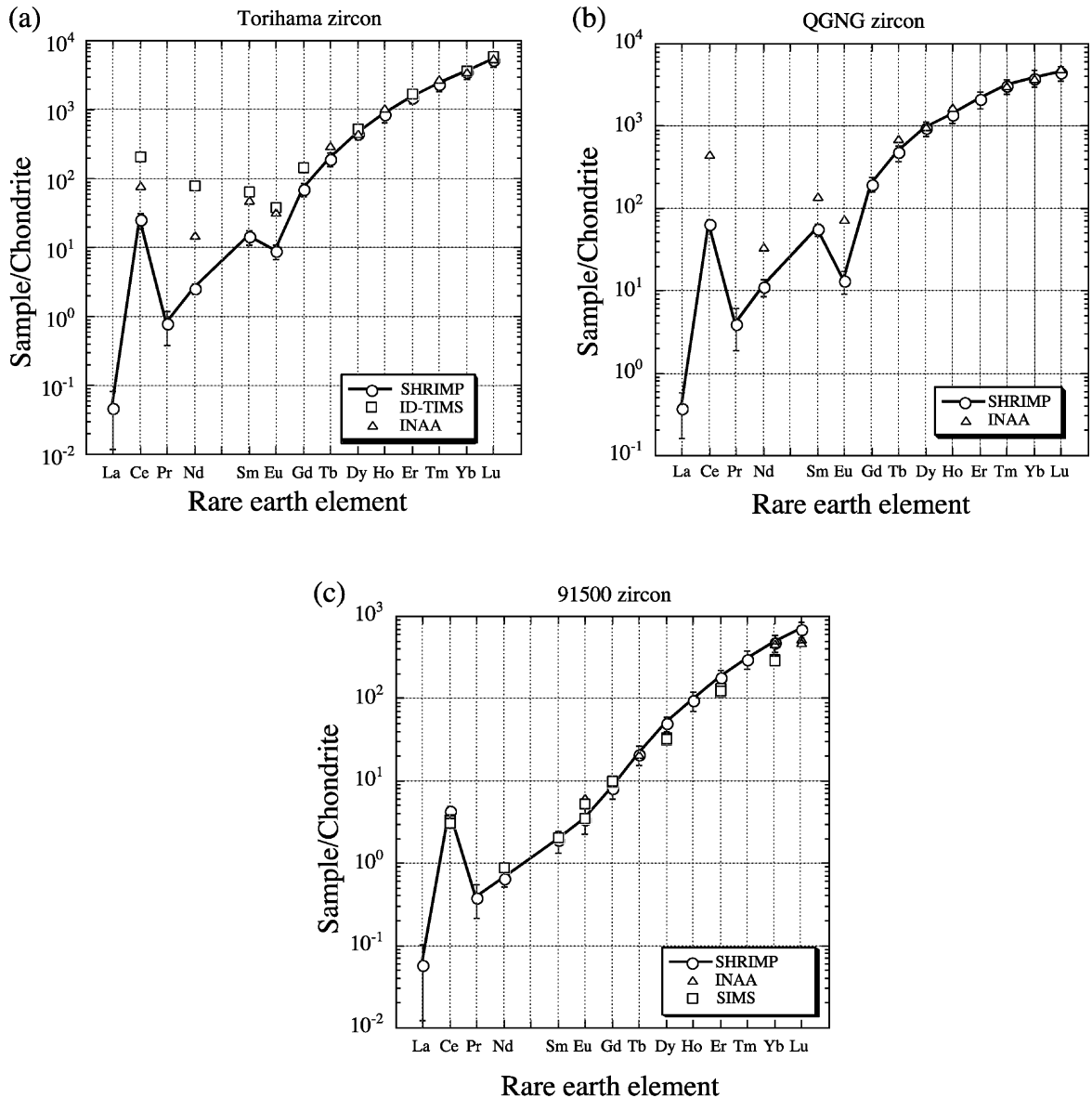


Fig. 2. (a) REE abundance patterns normalized to C1 chondrite in the Torihama zircon measured by SHRIMP (this work), ID-TIMS (Nagasawa, 1970) and INAA (this work). (b) The QGNG zircon measured by SHRIMP (this work) and INAA (this work). (c) The 91500 zircon measured by SHRIMP (this work), INAA (Wiedenbeck et al., 1995) and CAMECA 4f (Wiedenbeck et al., 1995). All errors are  $2\sigma$ .

where  $S$  is the secondary ion yield of REE indicated by the subscript. No correlation is apparent between the first valence and the relative secondary ion yields as reported by Reed (1983). Fig. 4 shows a relationship between the secondary ion yields for the REE (normalized to La) and the second ionisation potential.

The relative secondary ion yields decrease with increasing second ionisation potential. The trend illustrated by the dotted line in Fig. 4 is consistent with the relationship expected by on the basis of Eq. (2). However, the physical mechanism of this relationship is not well understood at present.

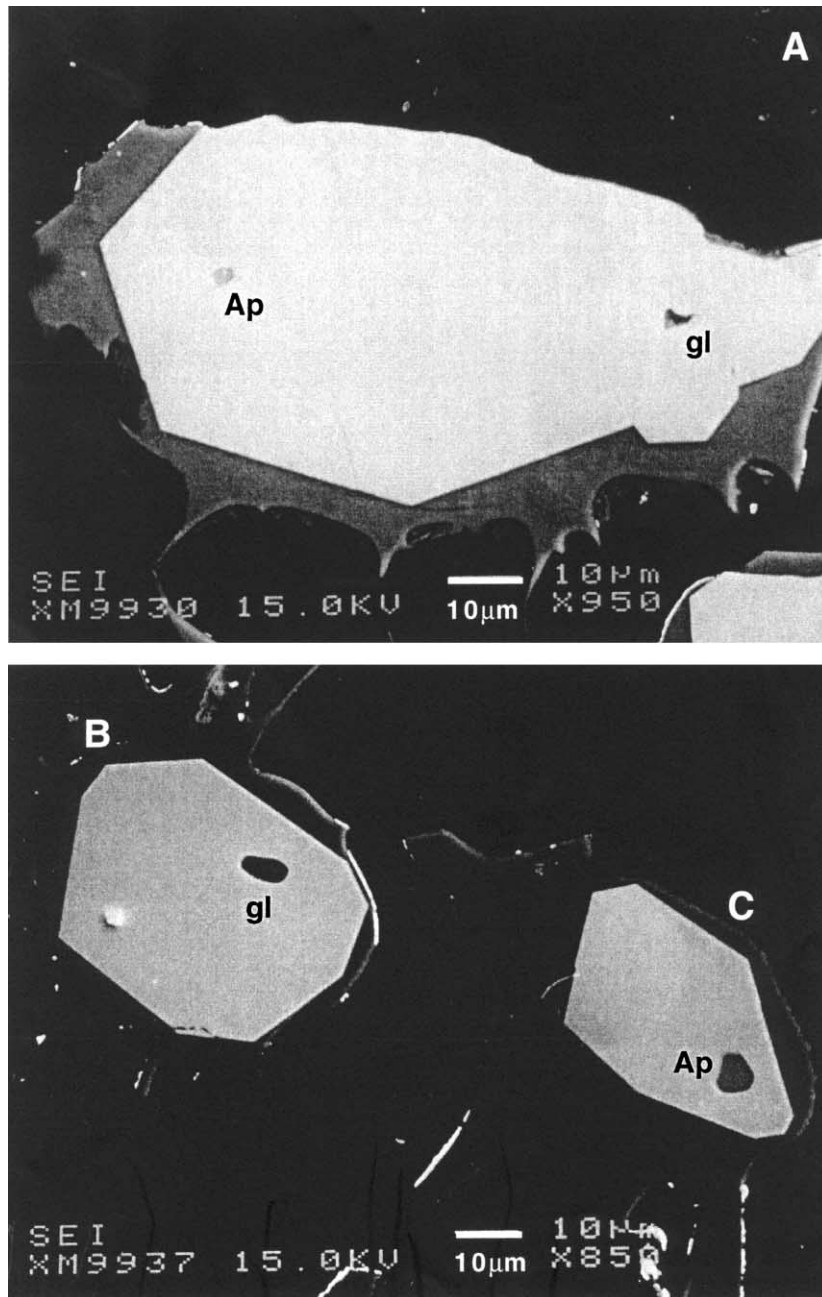


Fig. 3. Electron backscatter images of the Torihama zircon. Grain A contains both apatite and glass, while B and C include glass and apatite, respectively. The size of apatite inclusions varies from 1 to 5  $\mu\text{m}$ .

Fig. 5 shows the relationships between secondary ion yields of silicate glass and apatite, and of the glass and zircon. While errors for the LREE yields are

large, clear positive correlations exist for the data for the glass and the minerals. Since the chemical compositions of silicate glass, apatite and zircon differ

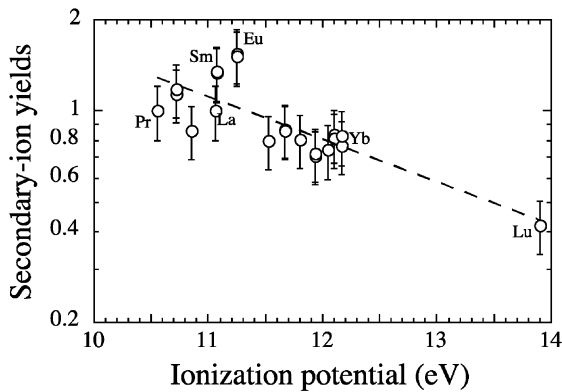


Fig. 4. A relationship between the secondary ion yields of REE and the ionisation potential of second valence (II), REE<sup>++</sup>. All errors are  $2\sigma$ .

significantly, the positive correlations in Fig. 5a and b indicate that the relative secondary ion yields of REE are not affected by matrices. Hitherto, it is well documented that such matrix effects are not always small. Shimizu (1978) reported that the sensitivity for Al relative to Si differs appreciably in different silicates. Steele et al. (1981) found that there are quite large variations in the secondary ion yields of major elements in olivines and low-Ca pyroxenes. In order to explain the matrix effect, Slodzian (1982) proposed a bond-breaking model for the ionization process, even though the model cannot predict the effect for complex samples quantitatively. Therefore, it is fully accepted that quantitative ion-probe analysis requires good calibration standards with approximate major chemistry to the samples. However, present REE data are independent from the matrix effect. This implies that REE patterns (not absolute abundances) in apatite and zircon could be determined by SIMS with reference to a glass standard rather than matrix-matched mineral standards. This is the most important finding of this work.

#### 4.3. Partition coefficients of REE in apatite/melt and zircon/melt

It is possible to calculate the apparent partition coefficients of REE between zircon and melt and/or apatite and melt when REE data for host rocks are available and mode of zircon is extremely small. Eight REE (Ce, Nd, Sm, Eu, Gd, Dy, Er, Yb and Lu)

concentrations in the groundmass samples of Torihama dacite pyroclastic pumice were reported by Nagasawa (1970), which is the host phase of apatite and zircon measured in this work. We have estimated contents of the other REE (La, Pr, Gd, Tb, Ho and Tm) by interpolation or extrapolation of the available REE in

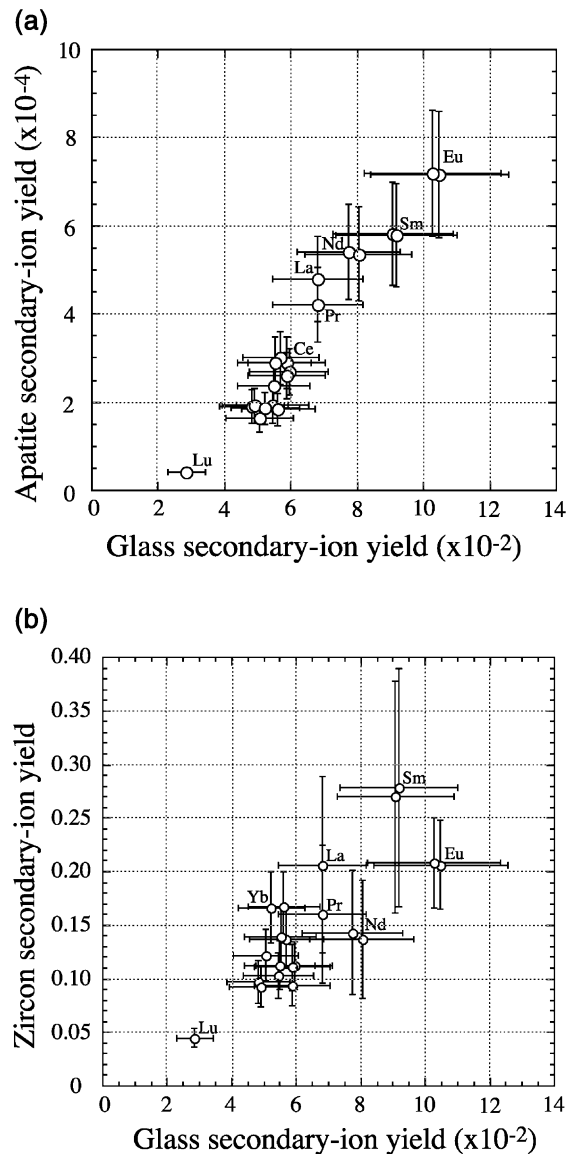


Fig. 5. (a) Comparison of REE secondary ion yields between silicate glass and apatite. (b) Comparison between silicate glass and zircon. All errors are  $2\sigma$ .

chondrite-normalized diagram. Partition coefficients of all REE were then calculated based on the observed REE in Torihama apatite and zircon, and REE of host dacite estimated above. Table 5 lists the coefficients of REE in apatite/melt and zircon/melt together with the ionic radius. Fig. 6 indicates a relationship between ionic radius of REE and the partition coefficients in apatite/melt and zircon/melt. The apatite partition coefficients define a concave shape with enrichment in the middle REE and a negative anomaly at Eu. This pattern is consistent with literature data (Nagasawa, 1970; Fujimaki, 1986) and may be of general applicability for intermediate- felsic volcanics. On the other hand, the zircon partition coefficients increase with increasing ionic radius. Anomalies at Ce and Eu may be due to the presence of  $Ce^{4+}$  and  $Eu^{2+}$  which have anomalous ionic radii. The zircon partition coefficients of light REE are different from those reported by bulk analyses while the heavy REE are almost consistent (Nagasawa, 1970; Fujimaki, 1986). This is probably attributable to the apatite or xenotime inclusion effects on bulk analysis. On the other hand the light REE are comparable with those reported by Hinton and Upton (1991) using SIMS while their heavy REE such as Tb, Dy, Ho and Er are somewhat discrepant from SHRIMP data. We cannot identify the reason for the difference in heavy REE coefficients. The zircon coefficients increase monotonically on a logarithmical scale (see Fig. 6), consistent with the power law dependency of

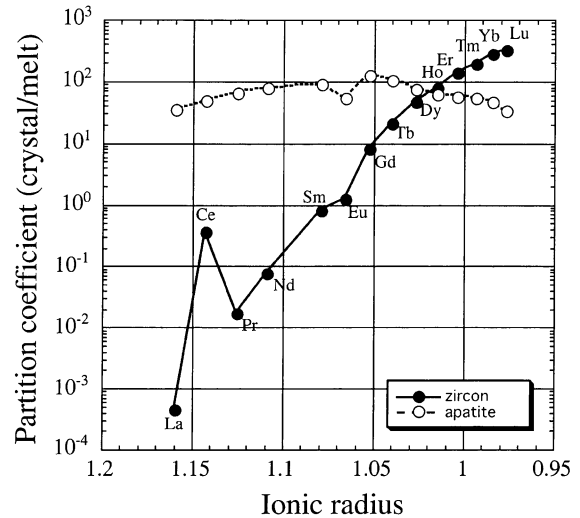


Fig. 6. A relationship between ionic radius of REE and partition coefficients of REE in zircon/melt and apatite/melt, respectively.

zircon/melt REE partitioning on the ionic radius (Hinton and Upton, 1991), the ionic radii of the REE decrease from  $La^{3+}$  to  $Lu^{3+}$  which should make REE substitution into the zircon lattice progressively easier for REE with higher atomic number.

The calculated REE partition coefficients (Table 5) can be used to estimate the REE concentrations in the melts coexisting with the zircon or apatite. The REE concentrations calculated are apparent estimates of the melt coexisting at the time of zircon or apatite growth. Such back-calculations are probably affected by other phases and any effects on partitioning due to physical and chemical changes. Hinton and Upton (1991) claimed that the estimate based on the zircon coefficients should give significant information on the REE pattern of the original melt. Recently, Hoskin et al. (2000) reported the REE abundances of accessory minerals extracted from adamellite and granodiorite in the Boggy Plain zoned pluton located in eastern Australia. Based on the REE of apatite, zircon and melt in sample BP11, and literature partition coefficients, they suggested that the back-calculation using apatite is successful while that using zircon does not match the REE pattern of the melt. They claimed that zircon REE characteristics are not as useful as a petrogenetic monitor. We have made such back-calculation using the zircon and apatite partition coefficients of REE in this work and data of BP11-a.2

Table 5  
Partition coefficients of REEs in apatite/melt and zircon/melt

Element	Ionic radius	Zircon/melt	Apatite/melt
La	1.160	$0.00046 \pm 0.00032$	$36 \pm 11$
Ce	1.143	$0.36 \pm 0.09$	$48 \pm 15$
Pr	1.126	$0.0172 \pm 0.0088$	$64 \pm 19$
Nd	1.109	$0.077 \pm 0.013$	$77 \pm 23$
Sm	1.079	$0.80 \pm 0.20$	$93 \pm 28$
Eu	1.066	$1.22 \pm 0.30$	$55 \pm 17$
Gd	1.053	$8.0 \pm 1.7$	$127 \pm 38$
Tb	1.040	$20.7 \pm 4.8$	$102 \pm 31$
Dy	1.027	$45.9 \pm 9.5$	$76 \pm 23$
Ho	1.015	$80 \pm 19$	$62 \pm 19$
Er	1.004	$136 \pm 27$	$57 \pm 17$
Tm	0.994	$197 \pm 40$	$53 \pm 16$
Yb	0.985	$277 \pm 55$	$48 \pm 14$
Lu	0.977	$325 \pm 62$	$33 \pm 10$

All errors are  $2\sigma$ .

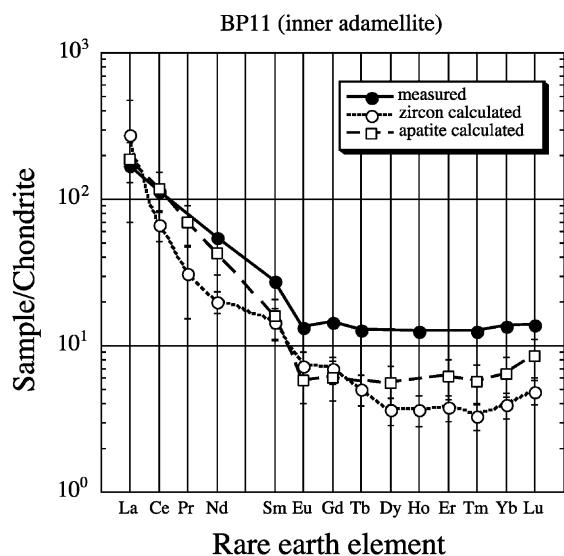


Fig. 7. REE abundance patterns normalized to C1 chondrite in measured BP11 melt referred from Hoskin et al. (2000) and those estimated by zircon and apatite back-calculation based on the partition coefficients obtained in this work. All errors are  $2\sigma$ .

zircon and BP11-2.1 apatite from Hoskin et al. (2000). Fig. 7 shows the comparison of measured and calculated melt composition for sample BP11. Both calculated melt REE patterns show strong LREE fractionation but essentially flat MREE and HREE. The patterns resemble that of the melt composition, suggesting that the previous report of partition coefficients of zircon/melt is incorrect and that zircon REE pattern can, in some cases, be used to reconstruct parental melt REE patterns.

## 5. Conclusions

An analytical procedure for all REE abundances in silicate glass, apatite and zircon minerals has been developed using the SHRIMP instrument with a high mass resolving power of 9300 at 1% peak height. The overall accuracy and precision are less than 30% at  $2\sigma$  for glass, apatite and heavy REE in zircon. The light REE contents in zircon are significantly smaller by the SHRIMP analysis than by the other methods such as INAA and ID-TIMS. The discrepancy is due to the presence of 1–5- $\mu\text{m}$  inclusions of apatite within a zircon grain.

Secondary ion yields of REE in a silicate glass show a negative correlation with the second valence ionization potential, which is consistent with a tendency expected by LTE model. The REE yields of glass agree well with those of apatite and zircon. The relative REE yields are probably not affected by matrix effect, suggesting that REE patterns in apatite and zircon could be determined by SIMS with reference to a glass standard. This is essential when the matrix-matched mineral standard is not available.

Partition coefficients of REE are estimated between melt and apatite, and melt and zircon based on data of the Torihama dacite. The zircon partition coefficients increase with increase of the ionic radius logarithmically, which was expected following the power law dependence of REE substitution into zircon lattice. Back-calculation of melt REE patterns by zircon and apatite and the partition coefficients generally work well in the Boggy Plain zoned pluton, suggesting both minerals are probably useful monitors in petrogenetic process.

## Acknowledgements

We are grateful to H. Shimizu, H. Hidaka and Y. Takahashi for discussions; Y. Tsutsumi for help in the laboratory; and K. Yokoyama and M. Shigeoka for EPMA analysis. We thank S.J.B. Reed, H. Yurimoto and C.V. Ly for critical readings of the manuscript. This is a contribution of a joint project between the SHRIMP laboratory at Hiroshima University and Center for Environmental Research at Ocean Research Institute, The University of Tokyo. **RD**

## References

- Anders, W., Grevesse, N., 1989. Abundances of the elements: meteoritic and solar. *Geochim. Cosmochim. Acta* 53, 197–214.
- Andersen, C.A., Hinthorne, J.R., 1973. Thermodynamic approach to the quantitative interpretation of sputtered ion mass spectra. *Anal. Chem.* 45, 1421–1438.
- Clauoué-Long, J.C., Compston, W., Roberts, J., Fanning, C.M., 1995. Two Carboniferous ages: a comparison of SHRIMP zircon dating with conventional zircon ages and  $^{40}\text{Ar}/^{39}\text{Ar}$  analysis. In: Berggren, A., Kent, D.V., Aubry, M.-P., Hardenbol, J. (Eds.), *Geochronology, Time Scales and Global Stratigraphic Correlation Society for Sedimentary Geology Special Publication* vol. 4, pp. 3–21.
- Eggins, S.M., Rundnick, R.L., McDonough, R.L., 1998. The com-

- position of peridotites and their minerals: a laser-ablation ICP-MS study. *Earth Planet. Sci. Lett.* 154, 53–71.
- Fahey, A.J., Goswami, J.N., McKeegan, K.D., Zinner, E., 1987.  $^{26}\text{Al}$ ,  $^{244}\text{Pu}$ ,  $^{50}\text{Ti}$ , REE and trace element abundances in hibonite grains from CM and CV meteorites. *Geochim. Cosmochim. Acta* 51, 329–350.
- Fujimaki, H., 1986. Partition coefficients of Hf, Zr and REE between zircon, apatite, and liquid. *Contrib. Mineral. Petrol.* 94, 42–45.
- Fukuoka, T., Arai, F., Nishio, F., 1987. Correlation of tephra layers in Antarctic ice by trace element abundances and refractive indices of glass shards. *Bull. Volcanol. Soc. Jpn.* 32, 103–118.
- Grandjean, P., Albarede, F., 1989. Ion probe measurement of rare earth elements in biogenic phosphates. *Geochim. Cosmochim. Acta* 53, 3179–3183.
- Gromet, L.P., Silver, L.T., 1983. Rare earth element distributions among minerals in a granodiorite and their petrogenetic implications. *Geochim. Cosmochim. Acta* 47, 925–939.
- Heaman, L.M., Bowins, R., Crocket, J., 1990. The chemical composition of igneous zircon suites: implications for geochemical tracer studies. *Geochim. Cosmochim. Acta* 54, 1597–1607.
- Hinton, R.W., Upton, B.G.J., 1991. The chemistry of zircon: variations within and between large crystals from syenite and alkali basalt xenoliths. *Geochim. Cosmochim. Acta* 55, 3287–3302.
- Hoskin, P.W.O., 1998. Minor and trace element analysis of natural zircon ( $\text{ZrSiO}_4$ ) by SIMS and laser ablation ICP-MS: a consideration and comparison of two broadly competitive techniques. *J. Trace Microprobe Tech.* 16, 301–326.
- Hoskin, P.W.O., Kinny, P.D., Wyborn, D., Chappell, B.W., 2000. Identifying accessory mineral saturation during differentiation in granitoid magmas: an integrated approach. *J. Petrol.* 41, 1365–1396.
- Ireland, T.R., Wlotzka, F., 1992. The oldest zircons in the solar system. *Earth Planet. Sci. Lett.* 109, 1–10.
- Jackson, S.E., Longerich, H.P., Dunning, G.R., Fryer, B.J., 1992. The application of laser-ablation microprobe-inductively coupled plasma-mass spectrometry (LAM-ICP-MS) to in situ trace-element determinations in minerals. *Can. Mineral.* 30, 1049–1064.
- Johnson, K.T.M., Dick, H.J.B., Shimizu, N., 1990. Melting in the oceanic upper mantle: an ion microprobe study of diopsides in abyssal peridotites. *J. Geophys. Res.* 95, 2661–2678.
- Kay, R.W., Gast, P.W., 1973. The rare earth content and origin of alkali-rich basalts. *J. Geol.* 81, 653–682.
- Kinny, P.D., Compston, W., Williams, I.S., 1991. A reconnaissance ion-probe study of hafnium isotopes in zircons. *Geochim. Cosmochim. Acta* 55, 849–859.
- Longerich, H.P., Jackson, S.E., Gunther, D., 1996. Laser ablation inductively coupled plasma mass spectrometric transient signal data acquisition and analyte concentration calculation. *J. Anal. At. Spectrom.* 11, 899–904.
- Maas, R., Kinny, P.D., Williams, I.S., Froude, D.O., Compston, W., 1992. The Earth's oldest known crust: a geochronological and geochemical study of 3900–4200 Ma old detrital zircons from Mt. Narryer and Jack Hills, Western Australia. *Geochim. Cosmochim. Acta* 56, 1281–1300.
- MacRae, N.D., Metson, J.B., 1985. In situ rare-earth element analysis of coexisting pyroxene and plagioclase by secondary ion mass spectrometry. *Chem. Geol.* 53, 325–333.
- Matsui, Y., Onuma, N., Nagasawa, H., Higuchi, H., Banno, S., 1977. Crystal structure control in trace element partition between crystal and magma. *Bull. Soc. Fr. Mineral. Cristallogr.* 100, 315–324.
- Metson, J.B., Bancroft, G.M., Nesbitt, H.W., Jonassen, R.G., 1984. Analysis for rare earth elements in accessory minerals by specimen isolated secondary ion mass spectrometry. *Nature* 307, 347–349.
- Murali, A.V., Parthasarathy, R., Mahadevan, T.M., Sankar Das, M., 1983. Trace element characteristics, REE patterns and partition coefficients of zircons from different geological environments—a case study on Indian zircons. *Geochim. Cosmochim. Acta* 47, 2047–2052.
- Nagasawa, H., 1970. Rare earth concentrations in zircons and apatites and their host dacites and granites. *Earth Planet. Sci. Lett.* 9, 359–364.
- Perkins, W.T., Pearce, N.J.G., Jeffries, T.E., 1993. Laser ablation inductively coupled plasma mass-spectrometry—a new technique for the determination of trace and ultra-trace elements in silicates. *Geochim. Cosmochim. Acta* 57, 475–482.
- Potts, M.J., Early, T.O., Herman, A.G., 1973. Determination of rare earth element distribution patterns in rocks and minerals by neutron activation analysis. *Z. Anal. Chem.* 263, 97–100.
- Reed, S.J.B., 1983. Secondary-ion yields of rare earths. *Int. J. Mass Spectrom. Ion Processes* 54, 31–40.
- Reed, W.P., 1992. Certificate of Analysis, Standard Reference Materials, 612, Trace Elements in a Glass Matrix. National Institute of Standards and Technology, Maryland, USA.
- Sano, Y., Terada, K., 2001. In situ ion microprobe U–Pb dating and REE abundances of a Carboniferous conodont. *Geophys. Res. Lett.* 28, 831–834.
- Sano, Y., Terada, K., Nishio, Y., Amakawa, H., Nozaki, Y., 1999a. Ion microprobe analysis of rare earth element in oceanic basalt glass. *Anal. Sci.* 15, 743–748.
- Sano, Y., Oyama, T., Terada, K., Hidaka, H., 1999b. Ion microprobe U–Pb dating of apatite. *Chem. Geol.* 153, 249–258.
- Shimizu, N., 1978. Analysis of the zoned plagioclase of different magmatic environments: a preliminary ion-microprobe study. *Earth Planet. Sci. Lett.* 39, 398–406.
- Shimizu, N., Richardson, S.H., 1987. Trace element abundance patterns of garnet inclusions in peridotite-suite diamonds. *Geochim. Cosmochim. Acta* 51, 755–758.
- Slodzian, G., 1982. Dependence of ionization yields upon elemental composition; isotopic variations. In: Benninghoven, A., Colton, R.J., Simons, D.S., Werner, H.W. (Eds.), *Secondary Ion Mass Spectrometry (SIMS III)*. Springer-Verlag, Berlin, pp. 115–123.
- Steele, I.M., Hervig, R.L., Hutcheon, I.D., Smith, J.V., 1981. Ion microprobe techniques and analysis of olivine and low-Ca pyroxene. *Am. Mineral.* 66, 526–546.
- Ui, T., 1971. Genesis of magma and structure of magma chamber of several pyroclastic flows in Japan. *J. Fac. Sci., Tokyo Univ., Sect. 2* 18, 53–127.
- Wiedenbeck, M., Alle, P., Crifu, F., Griffin, W.L., Meier, M., Oberli, A., Von Quadt, A., Roddick, J.C., Spiegel, W., 1995. Three

- natural zircon standards for U–Th–Pb, Lu–Hf, trace element and REE analyses. *Geostand. Newsl.* 19, 1–23.
- Zinner, E., Crozaz, G., 1986a. Ion probe determination of the abundances of all the rare earth elements in single mineral grains. In: Benninghoven, A., Colton, R.J., Simons, D.S., Werner, H.W. (Eds.), *Secondary Ion Mass Spectrometer (SIMS V)*. Springer-Verlag, Berlin, pp. 444–446.
- Zinner, E., Crozaz, G., 1986b. A method for the quantitative measurement of rare earth elements in the ion micro-probe. *Int. J. Mass Spectrom. Ion Processes* 69, 17–38.